Electronic Supplementary Material (ESI) for Energy & Environmental Science.

Formation of Lattice-dislocated Bismuth Nanowires on Copper Foam for Enhanced Electrocatalytic CO_2 Reduction at Low Overpotential

Xiaolong Zhang,[a] Xinghuan Sun,[a] Si-Xuan Guo,[a,b] Alan M. Bond,[a,b] Jie Zhang[a,b]*

[a]School of Chemistry, Monash University, Clayton 3800, Victoria, Australia.

[b]ARC Centre of Excellence for Electromaterials Science, Monash University, Clayton 3800, Victoria, Australia.

*Email: jie.zhang@monash.edu

Electronic Supporting Information

Preparation of H_2 and CO calibration curves.

The calibration curves of H_2 and CO were prepared as follows:

1. A known amount (n mol, n = 1.00×10^{-5}, 2.00×10^{-5}, 3.00×10^{-5}, 4.00×10^{-5}, and 5.00×10^{-5} mol) of CO or H_2 standard gas was injected into the same H cell used for bulk electrolysis with the same electrolyte solution volume and head space volume (the electrolyte solution was saturated with CO_2 and the head space is filled with pure CO_2).

2. The mixed gas in the head space of the H cell was then subjected to GC test to obtain the peak area value of CO or H_2.

3. Repeated experiments with different CO or H_2 amount were tested to obtain the calibration curves of CO and H_2. The amount of the injected CO or H_2 were plotted as a function of the corresponding peak area in GC. Calibration curves were obtained by linear fitting of the as-obtained data points (Figure S16).

The equation used to calculate FE of CO and H_2 is FE = (2*F*a*A)/C * 100%, where 2 is the number of electrons required per molecule to obtain CO or H_2, F is the Faraday constant, a is the slope value obtained from the calibration curves of CO or H_2, A is the peak area of CO or H_2 obtained from GC, and C is the total charges consumed during bulk electrolysis.

Calculation of overpotential

The equation used to calculate the overpotential of CO_2 reduction to formate is $\eta = | E - E^{0'}|$, where η is the overpotential, E is the actually applied potential, and $E^{0'}$ is the equilibrium potential for CO_2 reduction to formate. An $E^{0'}$ value of -0.09 V vs. RHE in a CO_2 saturated 0.5 M $NaHCO_3$ solution was estimated by us taking into account the pH dependent nature of carbonaceous and formate species (10.1016/j.nanoen.2016.11.004, supporting information). In this work, this $E^{0'}$

value was used for the calculation of overpotential. However, no IR calibration was applied to all the potential values reported in this work.

Figures and Tables

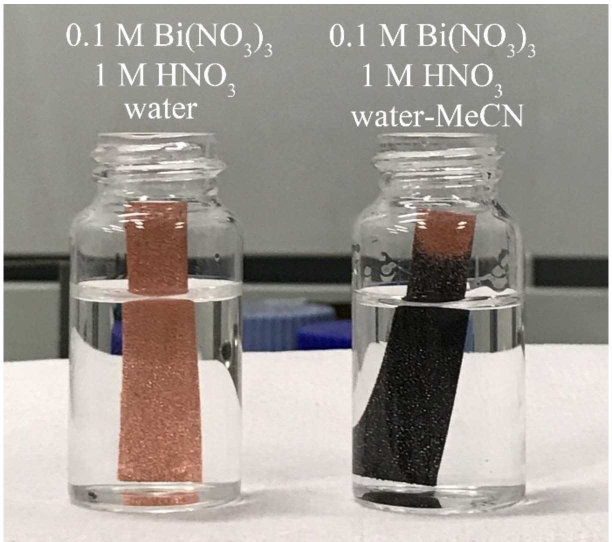

Figure S1. Photograph showing copper foams immersed in aqueous solutions containing 0.1 M $Bi(NO_3)_3$ and 1 M HNO_3 in the absence (left) and presence (right) of 50% MeCN for 5 seconds.

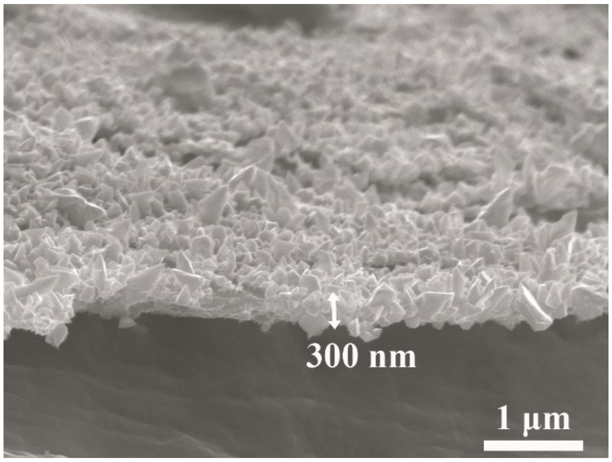

Figure S2. Cross-section view of the Bi layer coated on to copper foam.

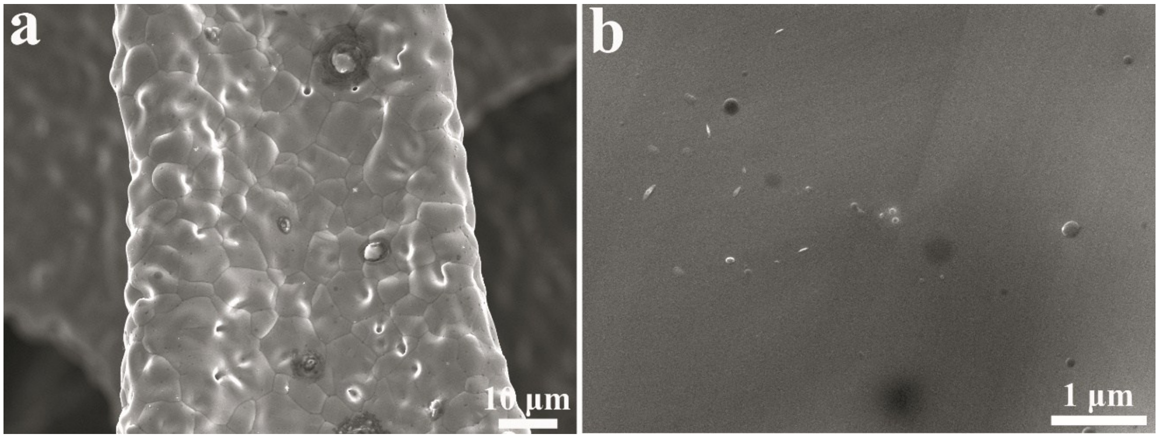

Figure S3. SEM images of a bare copper foam.

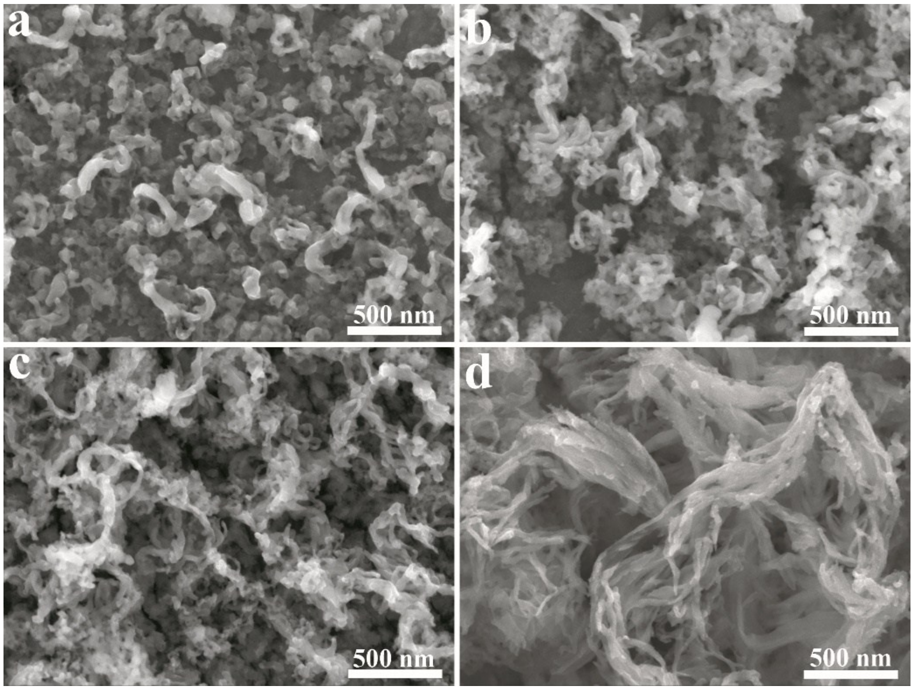

Figure S4. SEM images of Cu foam@Bi_2O_3 treated at -0.99 V for half hour and then treated at -0.69 V for (a) 0.5 h, (b) 1 h, (c) 2h, and (d) 4 h in a CO_2 saturated 0.5 M $NaHCO_3$ solution.

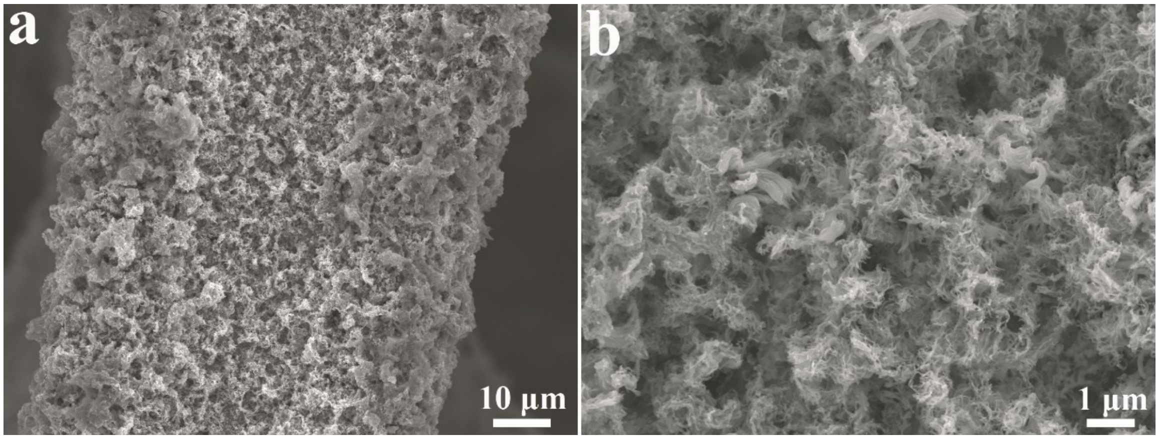

Figure S5. Low magnification SEM images of Cu foam@BNW.

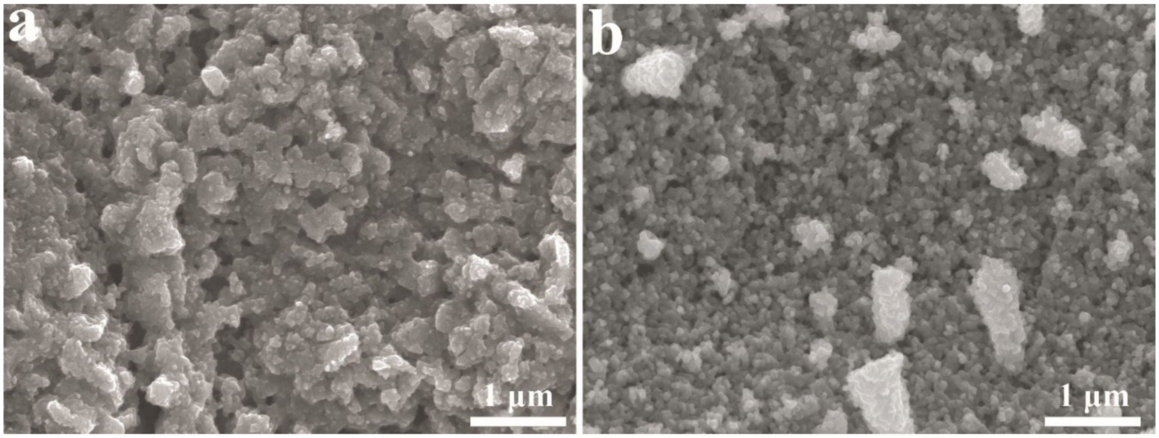

Figure S6. SEM images of Cu foam@Bi_2O_3 treated at (a) -0.99 V for half an hour and (b) -0.69 V for 4 hours in a CO_2 saturated 0.5 M $NaHCO_3$ solution.

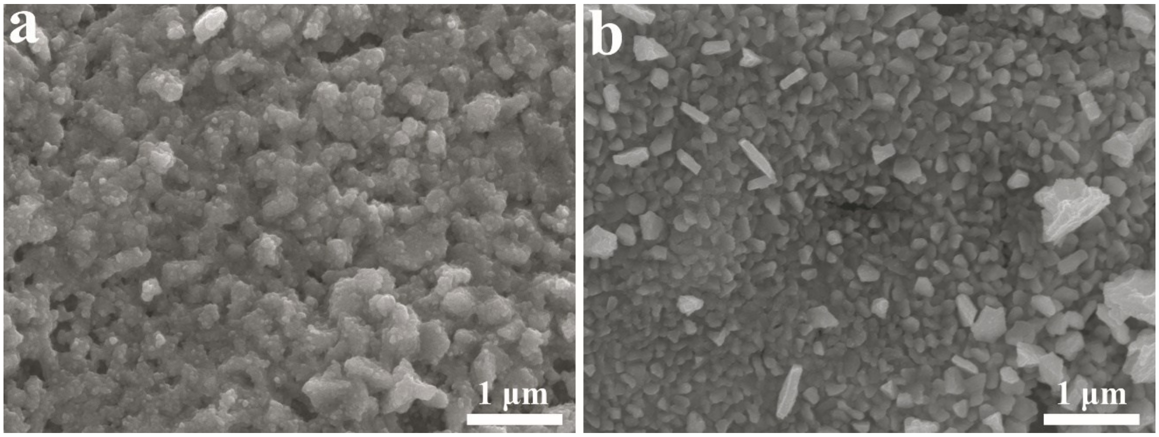

Figure S7. SEM images of (a) Bi plate@Bi_2O_3 treated at -0.99 V for half an hour and -0.69 V for 4 hours in a 0.5 M $NaHCO_3$ solution; (b) Cu foam@Bi_2O_3 treated at -0.99 V for half an hour and -0.69 V for 4 hours in a 0.5 M NaCl solution.

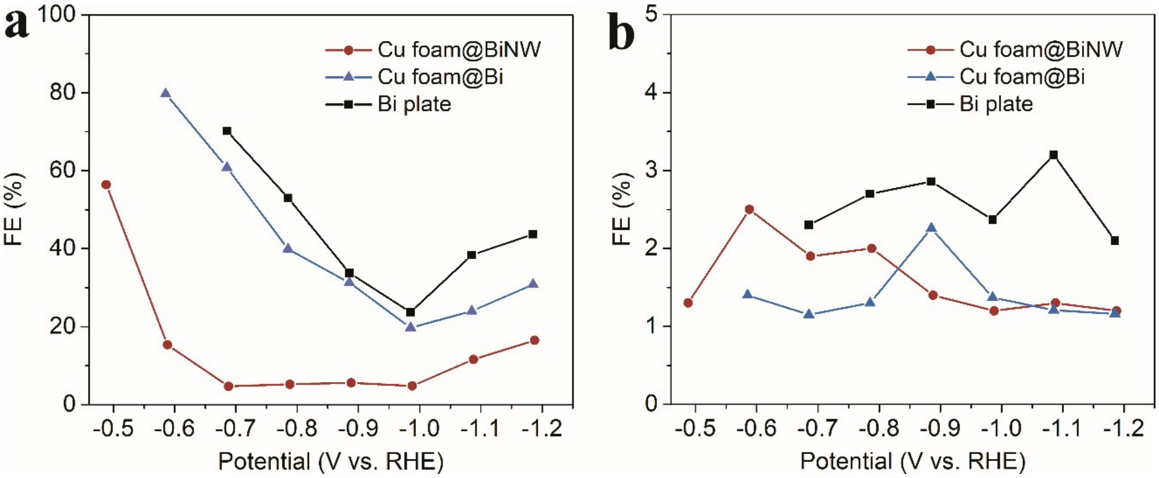

Figure S8. Faradaic efficiency distributions of (a) H_2 and (b) CO on Bi plate, Cu foam@Bi, and Cu foam@BiNW.

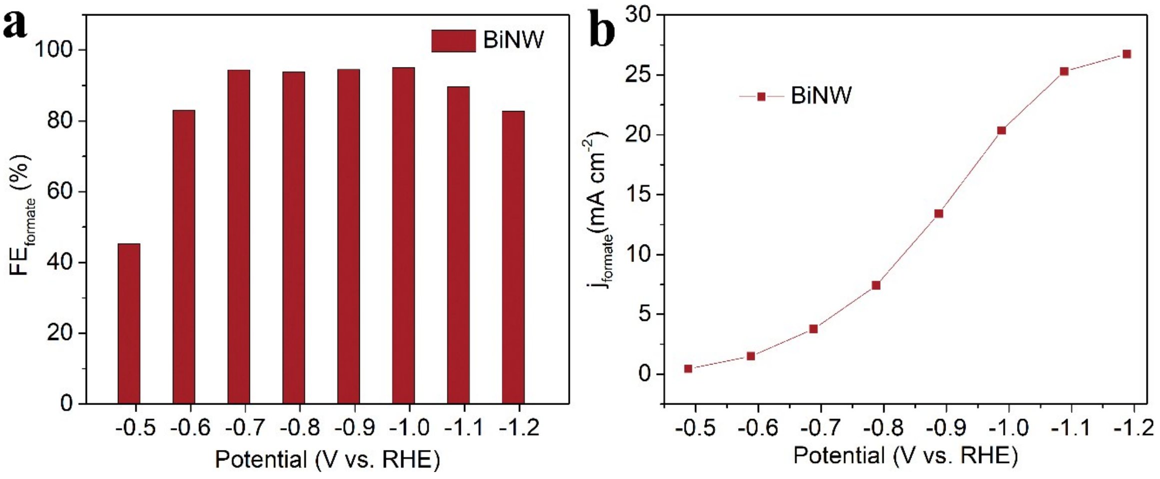

Figure S9. Bulk electrolysis results of the free standing BiNW peeled off from the Cu foam@BiNW electrode. The electrode substrate is a glassy carbon plate. (a) Faradaic efficiencies and (b) partial current densities for formate plotted as a function of applied potential.

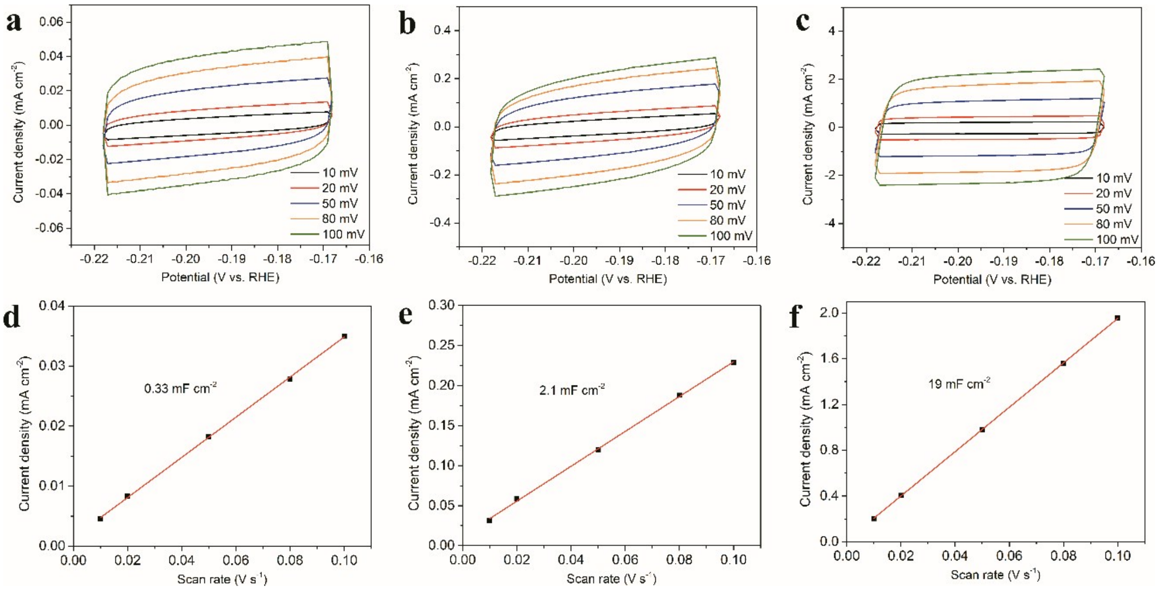

Figure S10. Double layer capacitance (C_{dl}) obtained from cyclic voltammogram (CV) measurements. CV curves of Bi plate (a), Cu foam@Bi (b) and Cu foam@BiNW (c) in CO_2 saturated 0.5 M NaHCO3 electrolyte between -0.218 V and -0.168 V vs. RHE. (d,e,f) The corresponding half of the charging current density difference plotted against scan rate. The linear slope is equivalent to the C_{dl}.

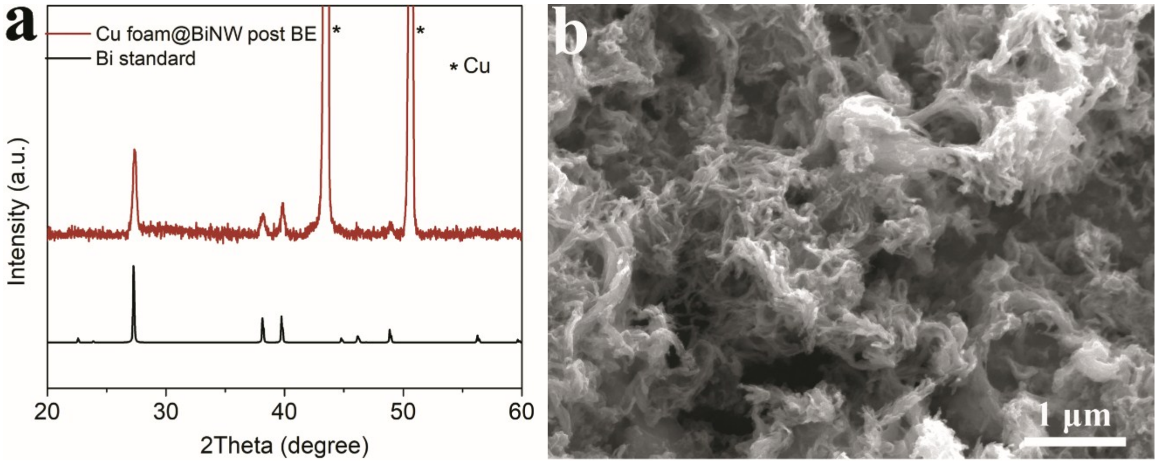

Figure S11. (a) XRD pattern and (b) SEM image of Cu foam@BNW obtained after long-term bulk electrolysis.

Table S1. List of $j_{formate}$ at -0.69 V vs.RHE, measured double layer capacitance, and jformate' per ECSA of the Bi plate, Cu foam@Bi and Cu foam@BiNW.

Sample name	**$j_{formate}$ at -0.69 V vs.RHE (mA cm^{-2})**	**C_{dl} (mF cm^{-2})**	**$j_{formate}$' at -0.69 V vs. RHE per ECSA (mA cm^{-2})**
Bi plate	0.13	0.33	0.39*α
Cu foam@Bi	0.77	2.1	0.37*α
Cu foam@BiNW	14.9	19	0.78*α

* $j_{formate}$' is calculated according to the following equation: $j_{formate}' = j_{formate}/Cdl*\alpha$. Where α (mF cm^{-2}) represents the specific capacitance of bismuth.

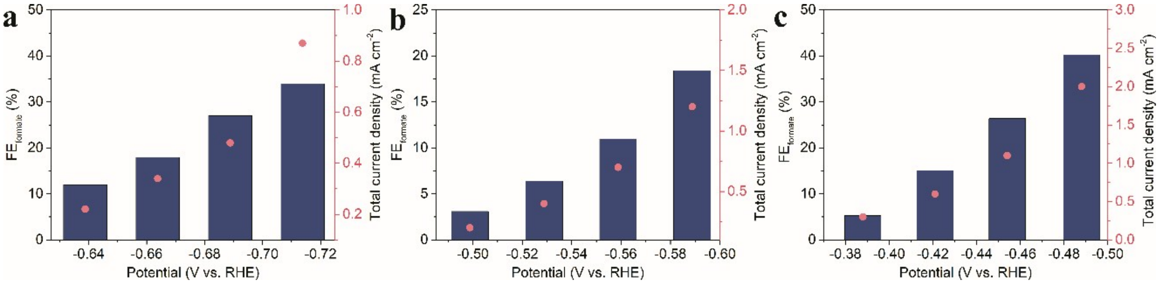

Figure S12. Extra bulk electrolysis results obtained on (a) Bi plate, (b) Cu foam@Bi and (c) Cu foam@BiNW in the low overpotential range where the reaction rate is kinetically controlled.

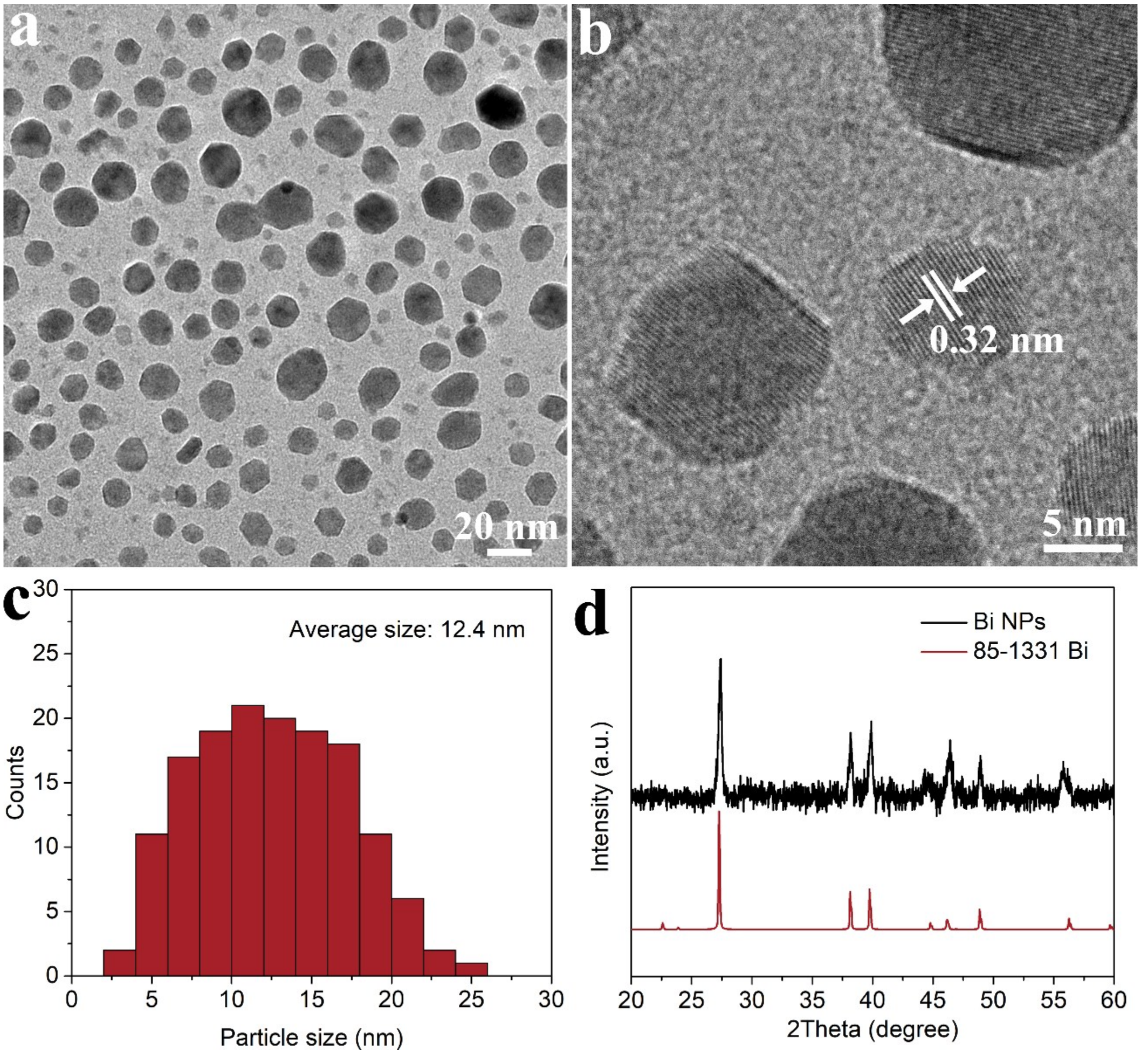

Figure S13. (a) TEM image, (b) HRTEM image, (c) particle size distribution, and (d) XRD pattern of the as-synthesized BiNPs with exposed (012) planes.

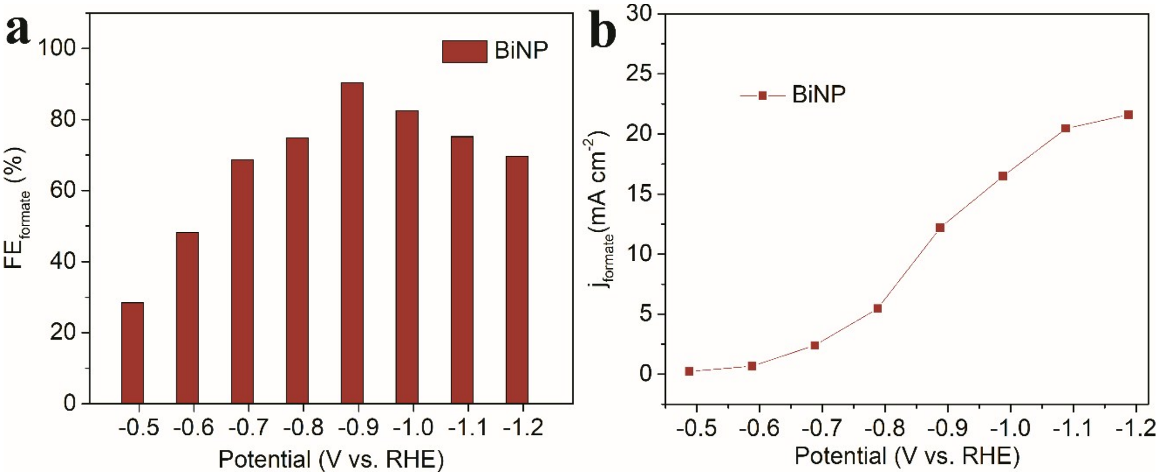

Figure S14. Bulk electrolysis results of the BiNPs. The electrode substrate is a glassy carbon plate. (a) Faradaic efficiencies and (b) partial current densities for formate plotted as a function of applied potential.

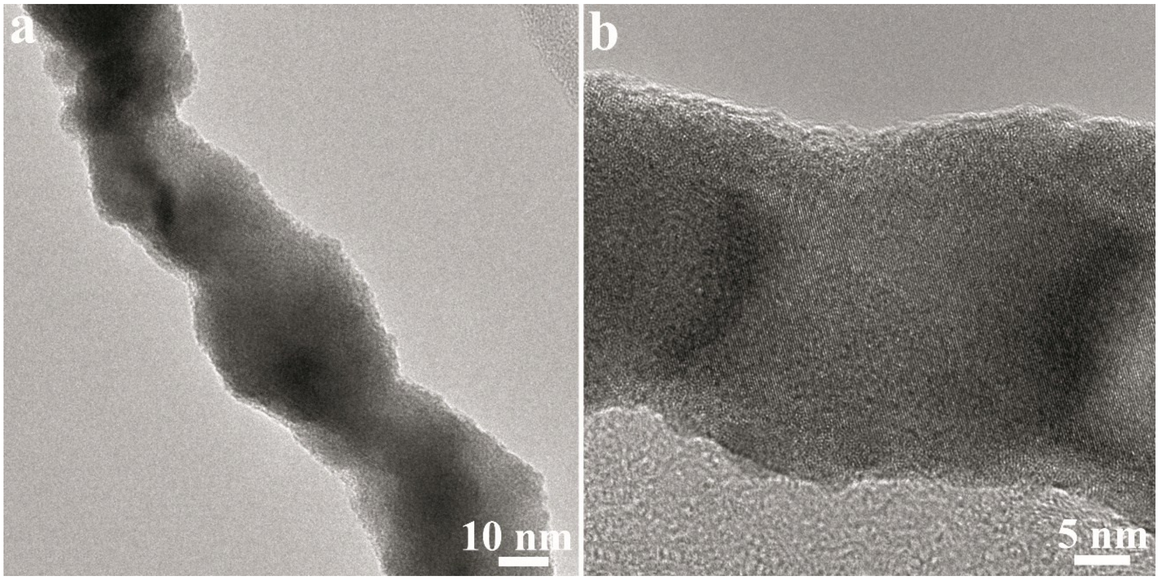

Figure S15. TEM images of a BiNW peeled off from a Cu foam@BNW electrode after long-term bulk electrolysis.

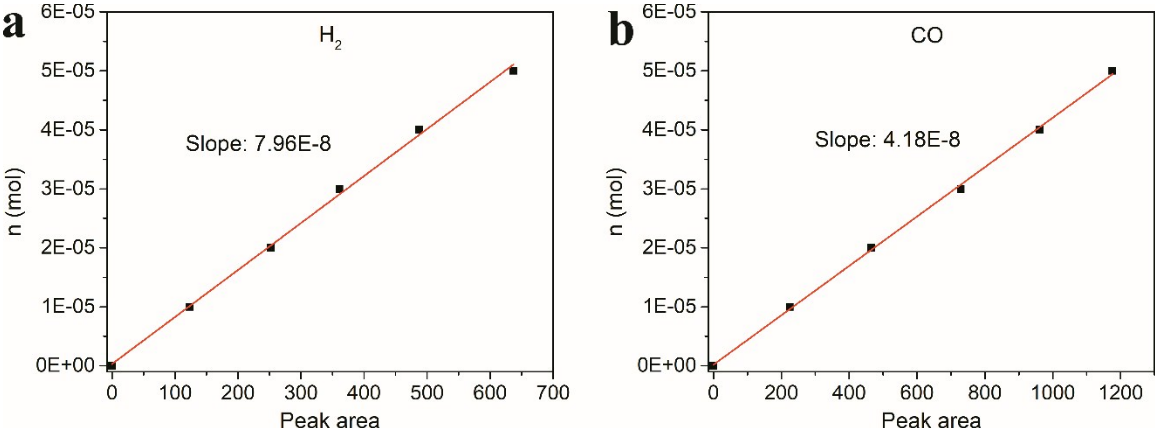

Figure S16. Calibration curves of (a) H_2 and (b) CO.

Table S2. Comparison of the electrocatalytic activity of the Cu foam@BiNW electrode with other state-of-the-art bismuth-based catalysts for electrocatalytic CO_2 reduction to formate in aquesou media.

Electrocatalysts	**Applied potential at maximum FE (V vs. RHE)**	**Maximum FE (%)**	**References**
Bi dendrite	-0.74	89	S1
BiO_x/C	-1.11	93.4	S2
BiNS	-0.86	95	S3
Bi_2O_3-NGQDs	-0.89	98.1	S4
	-1.19	90.8	
Bi-BiOC	-0.70	85	S5
Cu foam@BiNW	-0.69	95	This work
	-0.99	94	

References

S1. J. H. Koh, D. H. Won, T. Eom, N.-K. Kim, K. D. Jung, H. Kim, Y. J. Hwang and B. K. Min, *ACS Catal.*, 2017, **7**, 5071-5077.
S2. C. W. Lee, J. S. Hong, K. D. Yang, K. Jin, J. H. Lee, H.-Y. Ahn, H. Seo, N.-E. Sung and K. T. Nam, *ACS Catal.*, 2018, **8**, 931-937.
S3. N. Han, Y. Wang, H. Yang, J. Deng, J. Wu, Y. Li and Y. Li, *Nat. Commun.*, 2018, **9**, 1320.
S4. Z. Chen, K. Mou, X. Wang and L. Liu, *Angew. Chem. Int. Ed.*, 2018, **57**, 12790-12794.
S5. J. Zhang, Y. Zhang, X. Zhang, Y. Ling, F. Li and A. Bond, *Angew. Chem. Int. Ed.*, 2018, **57**, 13283-13287.